

Original Research

Netrin-1 Role in Nociceptive Neuron Sprouting through Activation of DCC Signaling in a Rat Model of Bone Cancer Pain

Zhihao Gong^{1,†}, Yuxin Zhang^{1,†}, Wei Wang^{1,†}, Xin Li^{1,2}, Kai Wang³, Xingji You^{2,*},
Jingxiang Wu^{1,*}¹Department of Anesthesiology, Shanghai Chest Hospital, Shanghai Jiao Tong University, School of Medicine, 200030 Shanghai, China²School of Medicine, Shanghai University, 200444 Shanghai, China³Central Laboratory, Shanghai Chest Hospital, Shanghai Jiao Tong University, School of Medicine, 200030 Shanghai, China*Correspondence: yoyo1976@shu.edu.cn (Xingji You); wjx1132@163.com (Jingxiang Wu)

†These authors contributed equally.

Academic Editor: Parisa Gazerani

Submitted: 24 August 2023 Revised: 13 September 2023 Accepted: 21 September 2023 Published: 27 February 2024

Abstract

Background: Bone cancer pain (BCP) is a common primary or metastatic bone cancer complication. Netrin-1 plays an essential role in neurite elongation and pain sensitization. This study aimed to determine the role of netrin-1 from the metastatic bone microenvironment in BCP development and identify the associated signaling pathway for the strategy of BCP management. **Methods:** The rat BCP model was established by intratibial implantation of Walker 256 cells. Von Frey filaments measured the mechanical pain threshold. Movement-induced pain was assessed using limb use scores. Expressions of associated molecules in the affected tibias or dorsal root ganglia (DRG) were measured by immunofluorescence, immunohistochemistry, real-time quantitative polymerase chain reaction, or western blotting. Transduction of deleted in colorectal cancer (DCC) signaling was inhibited by intrathecal injection of DCC-siRNA. **Results:** In BCP rats, the presence of calcitonin gene-related peptide (CGRP)-positive nerve fibers increased in the metastatic bone lesions. The metastatic site showed enrichment of well-differentiated osteoclasts and expressions of netrin-1 and its attractive receptor DCC. Upregulation of DCC and increased phosphorylation levels of focal adhesion kinase (FAK) and Rac family small GTPase 1/Cell division cycle 42 (Rac1/Cdc42) were found in the DRG. Intrathecal administration of DCC-siRNA led to a significant reduction in FAK and Rac1/Cdc42 phosphorylation levels in the DRG, decreased nociceptive nerve innervation, and improved pain behaviors. **Conclusions:** Netrin-1 may contribute to the activation of the BCP by inducing nociceptive nerve innervation and improving pain behaviors.

Keywords: bone cancer pain; netrin-1; DCC; FAK; Rac1/Cdc42; CGRP; axonal guidance; neurite elongation; nociception

1. Introduction

About 60–84% of patients with late-stage cancer experience different degrees of pain [1,2]. Currently, bone cancer pain (BCP) is primarily treated using a 3-step analgesic ladder, as the World Health Organization outlined in 1986. Additional therapies, such as radiation therapy, nerve lesions, osteoprotogerin, and diphosphonate, may also be utilized [1,3,4]. However, due to the complex and interactive nature of BCP mechanisms, the available treatment options are limited [1,5]. Therefore, it is crucial to gain a deeper understanding of the pathogenesis of BCP and explore alternative therapeutic targets for pain management.

BCP is believed to be caused by tumor-induced injury to sensory nerve fibers and abnormal sprouting of peripheral nociceptive nerve fibers in metastatic bone lesions [6,7]. Recently, nociceptive neurons in cancer-affected bones have displayed increased elongation and innervation. The majority of these sprouting nerve fibers are composed of calcitonin gene-related peptide (CGRP)-fiber and are connected to dorsal root ganglia (DRG). These fibers release CGRP from their central terminals in the dorsal horn [8]. Accumulative evidence has documented that bone tis-

sue is predominantly innervated by the peptide-rich CGRP + nerve fibers, which have been shown to participate in pain sensation [9–13]. The mechanisms leading to increased nociceptive nerve innervation at the site of bone metastases are poorly understood. In addition, the factors in the bone metastatic microenvironment that are thought to be involved in this pathological process require further investigation.

Netrin-1 is a neuronal guidance molecule that participates in developing the central nervous system and the regeneration of spinal cord and peripheral nerves [14,15]. It possesses multiple physiological functions such as axonal guidance [16,17], cell migration [18], morphogenesis [19], angiogenesis [20], and neuroinflammation [21]. Emerging studies have revealed the crucial role of netrin-1 in pain sensation by inducing the sprouting of nociceptive nerve fibers. Specifically, Wu *et al.* [14] demonstrated that netrin-1 increases deleted in colorectal cancer (DCC) expression in the spinal dorsal horn in resiniferatoxin-induced postherpetic neuralgia (PHN)-like rat model, contributing to mechanical hypersensitivity and sprouting of myelinated sensory fibers. Zhu *et al.* [22] proved that netrin-1 promotes sensory in-



nervation and osteoarthritis pain in an osteoarthritis mouse model. Moreover, Ni *et al.* [23] found that osteoclast-secreted netrin-1 initiates the porosity of endplates and sensory innervation in a lumbar spine instability (LSI) mouse model and contributes to spinal pain.

Secreted by multiple types of cells, such as neurons [24,25], macrophages [26], fibroblasts [27], and osteoclasts [22], netrin-1 accomplishes its physiological bi-functionality in nerve regeneration by binding to its canonical attractive receptors deleted in colorectal cancer (DCC) and neogenin or the repulsive DCC/uncoordinated (UNC5) A–D receptor complexes [17,28]. Subsequently, the downstream signal of netrin-1/DCC signaling is responsible for neurite elongation, the phosphorylation of focal adhesion kinase (FAK), and following phosphorylation of Rac family small GTPase 1/Cell division cycle 42 (Rac1/Cdc42) play critical roles in axon navigation [29,30].

As discussed previously, netrin-1 plays a potential role in developing and maintaining pain. In this study, we observed an elevated presence of CGRP + nerve innervation within the microenvironment of metastatic bone in a rat model of bone cancer pain (BCP), accompanied by a substantial differentiation of osteoclasts and expression of netrin-1. Furthermore, downstream netrin-1 signals, which promote neurite elongation through interaction with its attractive receptor DCC, were activated at the metastatic site and in the ipsilateral DRG of BCP rats. Subsequent knock-down of DCC via intrathecal injection of DCC-siRNA impeded the transduction of downstream signals associated with the netrin-1/DCC signaling pathway. It significantly alleviated the pain-related behaviors in BCP rats. These findings suggest that activating the netrin-1/DCC signaling pathway in cancer may subsequently contribute to an increased presence of nociceptive nerve fibers within the affected bone tissues, thereby contributing to the development of BCP.

2. Materials and Methods

2.1 Animals

Adult female Sprague-Dawley rats (6–8 weeks of age, Shanghai JieSiJie Laboratory Animals, Shanghai, China) were housed under standard laboratory conditions (light/dark cycle of 12/12 h, temperature 22–26 °C, humidity 55–60%) with water and food pellets available *ad libitum*. All experiments followed protocols approved by the Animal Care and Use Committee of Shanghai Chest Hospital, Shanghai Jiao Tong University, School of Medicine [permission no. KS (Y)20186] and the guidelines for investigations of experimental pain in animals published by the International Association for the Study of Pain [31].

2.2 Propagation of Walker256 Cells

Walker256 breast cancer cells (LLC-WRC 256, ATCC, Richmond, VA, USA), certified by short tandem repeat (STR) analysis and tested for mycoplasma con-

tamination, were cultured in a 6 mL medium containing M199 (M4530, Sigma Aldrich, Steinheim am Albuch, Germany), penicillin-streptomycin solution (100×) (C0222, Beyotime, Shanghai, China), and 5% horse serum (HS; 12449C, Sigma Aldrich, Steinheim am Albuch, Germany). Subculture was carried out twice a week when the cell density achieved 80%–90%. Heat-inactivated cells (10 min/95 °C) were used for sham group establishment. To confirm the efficiency of heat deactivation, deactivated cells were cultured and tested for proliferation after one day.

2.3 Rat BCP Model

The BCP model was developed by a single, well-trained male researcher utilizing a rat breast cancer cell line (Walker256 cells), as detailed earlier [32]. Briefly, rats were randomly grouped and received an injection of 10 µL of Walker256 cells (5×10^5 cells) (BCP group) into the lower third of the intramedullary canal of the right tibia using a 23-gauge needle under intraperitoneal pentobarbital anesthesia (2%, 40 mg/kg) (57-43-2, Sigma Aldrich, Steinheim am Albuch, Germany). Then, the syringe was removed, and bone wax was used to close the injection site. Erythromycin (E8100, Solarbio, Beijing, China) was used to prevent infection in the wound. The sham-treated group animals underwent the same procedures but were injected with heat-deactivated carcinoma cells instead of normal cells.

2.4 Behavioral Tests

One male observer was blinded to the experimental design for the duration of the entire study and administered all behavioral tests.

2.4.1 Paw Withdrawal Mechanical Threshold (PWMT) Test

A standard von Frey test was used to assess mechanical pain. Rats were placed in Individual translucent brown plastic cages (20 × 20 × 15 cm) on a metal mesh plate and allowed to adapt for 30 min. A von Frey monofilament was applied perpendicularly to the plantar surface of the hindpaw on the ipsilateral side of the lesions in ascending order of strength (0.6, 1.0, 1.4, 2, 4, 6, 8, 10, and 15 g) and held for 6–8 s until the paw was withdrawn. Each monofilament was applied five times at 5-min intervals. Brisk withdrawal or paw flinching was considered a positive response. The paw withdrawal mechanical frequency (PWMF) in response to each monofilament was calculated based on five applications. The paw withdrawal mechanical threshold (PWMT) was calculated as the force at which PWMF $\geq 60\%$. If PWMF $< 60\%$ for all filaments, 15 g was recorded as the PWMT [33].

2.4.2 Limb Use Score (LUS) Test

Movement-induced pain was estimated using limb use scores [11,33]. The rats were permitted to move sponta-

neously on a smooth plastic table (50 cm × 50 cm). Limb use during spontaneous ambulation was scored on a scale of 4 to 0 (4, normal; 3, slight limp; 2, obvious limp; 1, partial use of limbs; 0, no use of limbs).

2.5 Bone Histomorphometric Analysis

The ipsilateral tibia of BCP rats was fixed in 4% paraformaldehyde (P1110, Solarbio, Beijing, China) for 48 h, then decalcified in 10% ethylenediamine tetraacetic acid (EDTA; G1105, Servicebio, Wuhan, China) for 3–4 weeks, and 6- μ m sections were cut using a rotating microtome. Paraffin-embedded sections were deparaffinized in xylene and rehydrated. Hematoxylin–eosin (H&E; GP1031, Servicebio, Wuhan, China) and Tartrate-resistant acid phosphatase (TRAP; G1050, Servicebio, Wuhan, China) staining were conducted according to the manufacturer's protocol.

2.5.1 Micro-Computerized Tomography (Micro-CT)

The tibias of sham-treated and BCP rats were collected and scanned with a VivaCT 80 scanner with a 55-kVp source (Scanco, Southeastern, PA, USA). The area of interest was the proximal 1/3 of the tibias. Images and parameters were acquired for 3D reconstruction, such as bone volume/total volume (BV/TV) and connectivity density (Conn.D.), using Scanco Medical software (Scanco mCT 40; SCANCO Medical AG, Bruttisellen, Switzerland).

2.5.2 Immunofluorescent Staining

The paraffin-embedded sections were deparaffinized in xylene (G1128, Servicebio, Wuhan, China) and rehydrated. Antigen retrieval was performed with protease K (G1234, Servicebio, Wuhan, China) at 37 °C for 15 min. Then the sections were permeabilized in 0.3% Triton X-100 solution (P0096, Beyotime, Shanghai, China) for 10 min, blocked with blocking solution (5% BSA (GC305006, Servicebio, Wuhan, China) and 10% goat serum (G1208, Servicebio, Wuhan, China)) for 1 h and finally incubated with primary antibodies against CGRP (1:100, sc-57053; Santa Cruz Biotechnology, Santa Cruz, CA, USA), netrin-1 (1:100, PA5-95725, Invitrogen, Carlsbad, CA, USA), DCC (1:1000, ab273570; Abcam, Cambridge, UK) and secondary antibody (1:500) (catalog nos. #4412 and #8890, Cell Signaling Technology, Boston, MA, USA) in the dark. Then an antifade mounting medium containing 4',6-diamidino-2-phenylindole (DAPI; P0131, Beyotime, Nanjing, China) was used. Images were acquired using a confocal laser scanning microscope (Leica Microsystems, Mannheim, Germany). Quantitative histomorphometric analysis was blinded using a public domain, Java-based image processing software (ImageJ, Version 2.0.0-rc-69/1.52p, <https://imagej.net/>). We collected and evaluated the mean CGRP density in 5 slices of the tibial marrow area on the slide for each specimen in each group.

2.5.3 Immunohistochemical Staining

The paraffin-embedded sections were deparaffinized in xylene and rehydrated. Antigen retrieval was performed with protease K at 37 °C for 15 min. The activity of endogenous peroxidase was blocked with a 3% H₂O₂ solution. The samples were stained overnight at 4 °C with mouse monoclonal antibody against CGRP (1:100, sc-57053; Santa Cruz Biotechnology, Santa Cruz, CA, USA) or rabbit polyclonal antibody against netrin-1 (1:100, PA5-95725, Invitrogen, Carlsbad, CA, USA). After washing three times with phosphate-buffered saline (PBS), horseradish peroxidase-conjugated secondary antibodies (1:200, G1213, G1214, Servicebio, Wuhan, China) were added and incubated for 1 h at room temperature. Negative control experiments were carried out by omitting the primary antibodies. 3,3'-diaminobenzidine (DAB; G1212, Servicebio, Wuhan, China) was used as a chromogen, and hematoxylin (GP1031, Servicebio, Wuhan, China) was used to counterstain. The sections were examined using a microscope (Carl Zeiss Microscopy GmbH 37081, Göttingen, Germany).

2.6 RNA Extraction and Real-Time Quantitative PCR (RT-qPCR)

Total RNA was isolated from L3-L5 DRGs (thereafter DRG) using the RNA-easy Isolation Reagent (R701, Vazyme Biotech, Nanjing, China), and complementary DNA (cDNA) was generated using a cDNA Synthesis Kit (DBI-2220, DBI® Bioscience, Ludwigshafen, Germany). RT-qPCR was performed using a Quantitect SYBR Green kit (DBI-2043, DBI® Bioscience) on a StepOne-Plus™ Real-Time PCR System (Applied Biosystems®, Thermo Fisher Scientific, Waltham, MA, USA). The following primers were used in the study: DCC sense: 5'-CTCGGAATCCAGCCAGCACAAG-3', DCC antisense: 5'-AACACAACACTCCAGGACAGCATC-3'; UNC5B sense: 5'-GCCGAGCCTACATCCGCATTG-3', UNC5B antisense: 5'-GCCATTCCACCTCAGCCACAG-3'; GAPDH sense: 5'-GGTGGACCTCATGGCCTACA-3', GAPDH antisense: 5'-CTCTCTTGCTCTCAGTATCCTTGCT-3'. The level of the target mRNA was quantified relative to the housekeeping gene (GAPDH) using the $2^{-(\Delta\Delta Ct)}$ method [34].

2.7 Western Blotting

The DRG lysates were centrifuged, and the supernatants were separated by sodium dodecyl sulfate polyacrylamide gel electrophoresis (SDS-PAGE) and blotted on polyvinylidene fluoride membranes (Pall Medical, Ann Arbor, MI, USA). The membranes were blocked with 5% milk in tris-buffered saline Tween-20 (TBST) at room temperature for 2 h and probed with primary antibodies overnight at 4 °C. The following primary antibodies were used: DCC (1:1000, ab273570; Abcam), UNC5B (1:1000, #13851; Cell Signaling Technology, Danvers, MA, USA), FAK

(1:1000, #3285; Cell Signaling Technology), Phospho-FAK (Tyr397) (1:1000, #3283, Cell Signaling Technology), Rac1/Cdc42 (1:1000, #4651; Cell Signaling Technology), Phospho-Rac1/Cdc42 (Ser71) (1:1000, AF2393; Affinity Biosciences, Columbus, OH, USA) and GAPDH (1:2000, BL006B; Biosharp Life Sciences, Hefei, Anhui, China). The membranes were washed in TBST for 3 times and incubated for 1 h at room temperature with HRP-coupled anti-rabbit IgG secondary antibody (1:2000, #7074; Cell Signaling Technology). Finally, the membranes were identified using a computerized image analysis system (Chem-Doc XRS1, Bio-Rad, Hercules, CA, USA). The intensity of the protein bands was quantified using Image Lab software (ImageJ, Version 2.0.0-rc-69/1.52p, <https://imagej.net/>). The expression of target proteins was normalized against that of glyceraldehyde-3-phosphate dehydrogenase (GAPDH).

2.8 Knockdown of DCC in the DRG of the BCP Model

Three siRNAs were designed to knock down the expression of DCC (GenePharma, Shanghai, China). Sequences of these siRNAs were: DCC-281-siRNA sense: 5'-GGGUCUCUGUUGAUACAAATT-3', DCC-281-siRNA antisense: 5'-UUUGUAUCAACAGAGACCCTT-3'; DCC-924-siRNA sense: 5'-CGUGCGUUGUCACAU AUAATT-3', DCC-924-siRNA antisense: 5'-UUAUAUG UGACAACGCACGTT-3'; DCC-2356-siRNA sense: 5'-G GAGUCGAGUUCUCAUAUTT-3', DCC-2356-siRNA antisense: 5'-AUAUGAGAACUCGACUCCTT-3'. Pilot experiments showed that the DCC-281-siRNA sequence achieved the greatest knockdown efficiency when injected intrathecally into naïve rats (**Supplementary Fig. 1**, n = 8 per group). Therefore, it was used in all subsequent experiments.

Rats were randomly divided into groups that received an intrathecal administration of 2 µg DCC siRNA in 10 µL of *in vivo*-jetPEI™ (201-10G, Polyplus-transfection, Illkirch, France) or 10 µL of *in vivo*-jetPEI™ only on days 10, 13, and 16 under light anesthesia with sevoflurane (n = 12 per group). The animals underwent behavioral assessments just before the commencement of the study, on the initial day of the intervention, and subsequently daily throughout the duration of the intervention. Upon completing the experiments on the seventeenth day, DRG samples and ipsilateral tibial bones were collected for further analysis.

2.9 Statistical Analysis

Results of behavior tests are expressed as median ± 95% confidence interval; other results are expressed as mean ± standard deviation. The data were analyzed using GraphPad Prism 8.0 for Windows (GraphPad, San Diego, CA, USA). All behavioral tests and other experiments were performed in a blinded manner. Data from behavioral tests were analyzed using two-way repeated-measures analysis of variance (ANOVA), followed by Tukey's post hoc

test. For other data, comparisons between two groups were analyzed using two-tailed unpaired Student's *t*-tests or Wilcoxon-Mann-Whitney tests, and comparisons among more than three groups were analyzed using one-way ANOVA followed by Tukey's post hoc test. Differences for which the *p*-value was smaller than 0.05 were considered statistically significant.

3. Results

3.1 Intratibial Inoculation of Walker256 Cells Results in Pain Behavior and Bone Loss in Recipient Rats

To elucidate the inoculation of Walker256 cells that resulted in pain behaviors and bone loss, pain behavior tests were performed on days 0, 4, 7, 11, 14, 17, and 21 (Fig. 1A). The paw withdrawal mechanical threshold (PWMT) and the limb use score for the BCP group decreased significantly following the disease progression (Fig. 1B,C). On day 21, the tibias of rats treated with BCP revealed apparent bone mass loss, whereas sham-treated rats exhibited no discernible bone loss (Fig. 1D, arrows). In the meantime, hematoxylin and eosin staining of the tibial sections showed notable osteolytic lesions with fractures along the cortical shaft of tibias from BCP rats (Fig. 1E, arrows). Moreover, the micro-CT images demonstrated a notable decline in bone mass in the tibias of BCP rats compared to the sham-treated rats. Additionally, a considerable decrease in the cortical bone volume/total volume (BV/TV) and the trabecular bone connectivity density (Conn D.) were verified through data analysis (Fig. 1F). These results indicate that the BCP model was established successfully.

3.2 Nociceptive Nerve Innervation of the Affected Tibias Increases during the Development of Bone Cancer

We examined the nociceptive nerve fibers that innervate the affected tibias by immunostaining CGRP. Compared to sham-treated rats, the innervation and density of CGRP + nociceptive nerve fibers increased in the tibias of rats with BCP (Fig. 2A,B). In addition, the immunohistochemistry staining revealed abnormal CGRP + nociceptive nerve fiber distribution (Fig. 2C, yellow arrows) near the trabecular bone surface. This was accompanied by significant multinuclear osteoclast activation, as confirmed by TRAP staining (Fig. 2C, blue arrows) in the ipsilateral tibias of BCP rats compared to sham-treated rats. These results suggest an increase in the innervation of CGRP + nociceptive nerve fibers in the affected tibias of BCP rats, which plays an important role in abnormal nociception during the development of hyperalgesia.

3.3 Sprouting of CGRP-Positive Fibers in Metastatic Bone Lesions is Associated with Increased Expression of Osteoclast-Derived Netrin-1

Recently, Zhu *et al.* [22] demonstrated that osteoclast-derived netrin-1 is important in regulating osteoarthritis pain. It is known that activated osteoclasts in the microenvi-

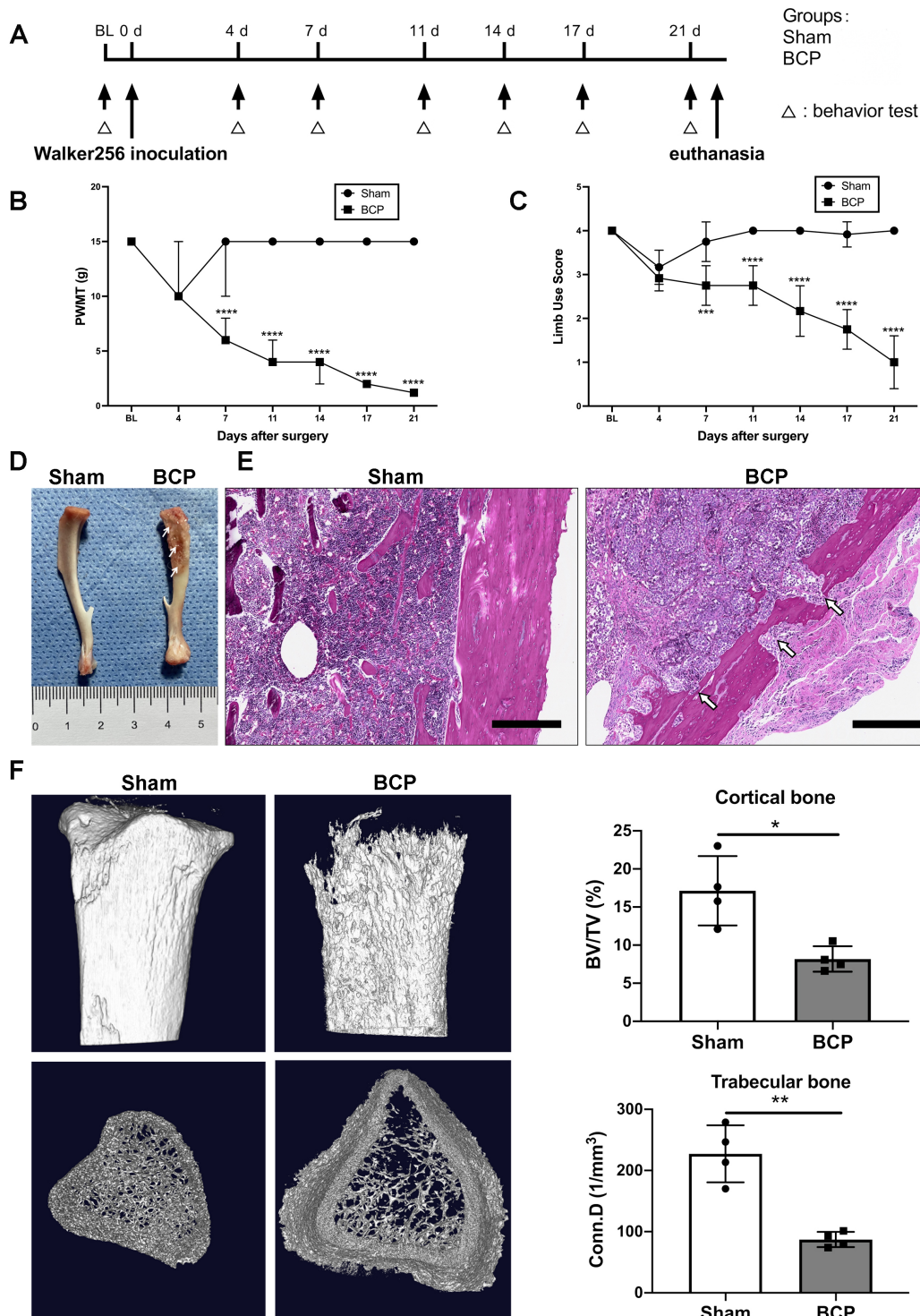


Fig. 1. Intratibial inoculation of Walker256 mammary gland carcinoma cells leads to pain behaviors and bone loss in rats. (A) Timeline of the experimental schedule. (B) PWMT and (C) limb use score for pain behavior tests in sham and BCP groups. $n = 12$ per group. Data are expressed as median \pm 95% CI. $***p < 0.001$, $****p < 0.0001$. (D) Anatomic structure of tibia bone from sham and BCP rats on day 21 post-inoculation of Walker256 cancer cells. (E) Histological sections (hematoxylin and eosin-stained) showed obvious medullary and cortical bone loss on day 21. Scale bars, 400 μm . (F) Representative micro-CT reconstruction images of the proximal tibias from the sham and BCP groups. Morphometric parameters, including BV/TV and Conn.D. $n = 4$ per group. Data are expressed as mean \pm standard deviation (SD). $*p < 0.05$, $**p < 0.01$, $****p < 0.0001$. BL, baseline; BCP, bone cancer pain; PWMT, paw withdrawal mechanical threshold; Conn.D., connectivity density; BV/TV, bone volume/total volume; 95% CI, 95% Confidence Interval.

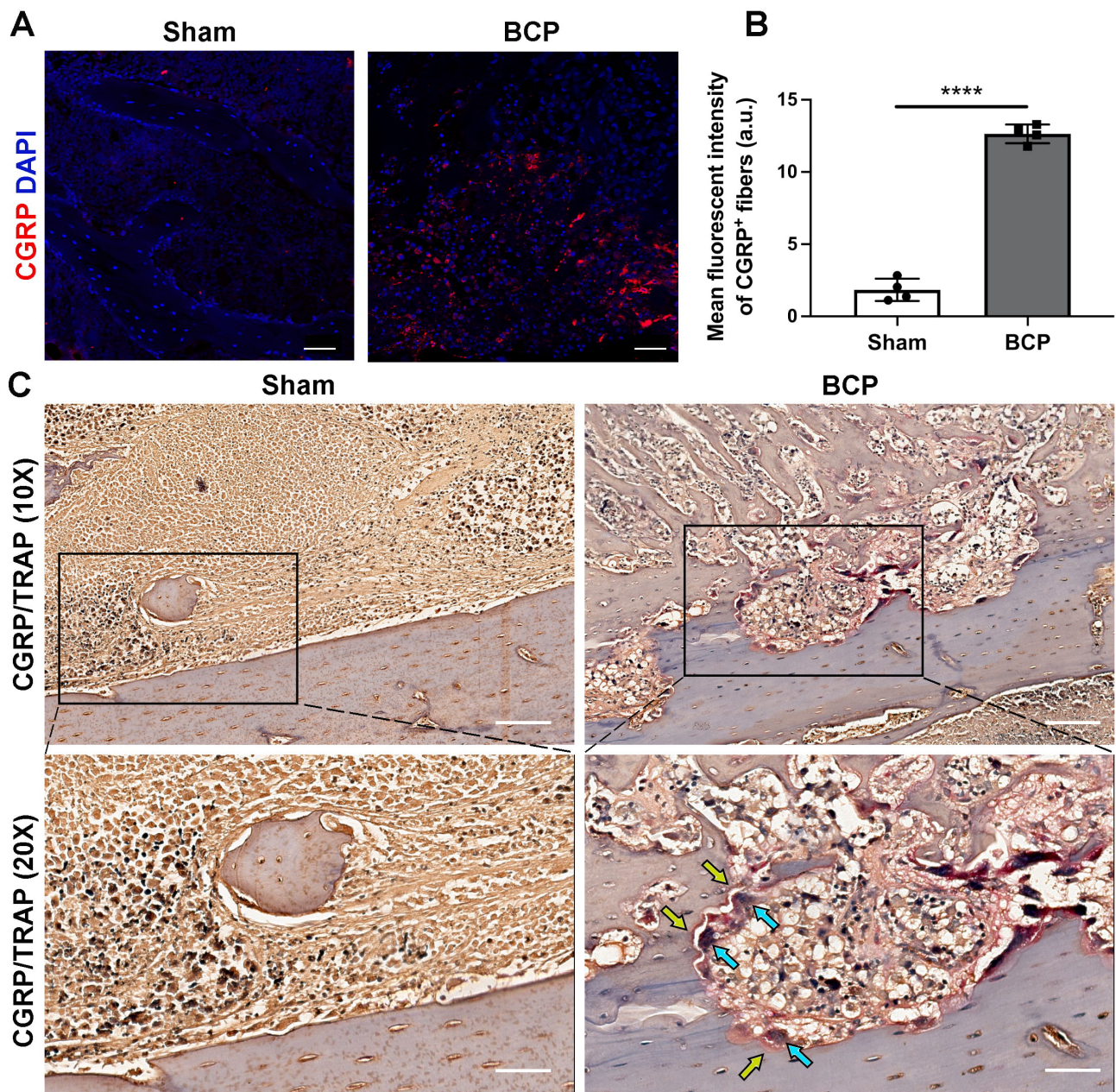


Fig. 2. Innervation of CGRP + nociceptive nerve fibers increased in the affected tibias during BCP progression. (A) Immunofluorescence analysis of CGRP + nociceptive nerve fibers (red) in the tibias on day 21 after Walker256 cell inoculation. Scale bars, 50 μm . (B) Quantitative analysis of the mean density of CGRP + sensory nerve fibers in panel A, $n = 4$ per group. (C) Representative images of CGRP + nerve fibers (yellow arrows) and TRAP + osteoclasts (blue arrows) staining in the tibias of sham-treated and BCP rats on day 21, $n = 4$ per group. Scale bars, 200 μm (10 \times); 100 μm (20 \times). Data are expressed as mean \pm SD. **** $p < 0.0001$. CGRP, calcitonin gene-related peptide; TRAP, Tartrate-resistant acid phosphatase.

ronment of bone metastasis are critical for the initiation and development of BCP [1,35]. Consistent with this evidence, we detected activation of osteoclasts by TRAP staining (blue arrows) along with upregulation of netrin-1 (yellow arrows) in the affected tibias of BCP rats (Fig. 3A). Meanwhile, immunofluorescent staining showed prominent upregulation of netrin-1 expression in the affected tibias of BCP rats compared with sham-treated rats (Fig. 3B,C). Furthermore, double immunofluorescent staining showed spa-

tial proximity of netrin-1 and CGRP expressions in the affected tibias of BCP rats (Fig. 3B). These findings imply that in the metastatic bone lesions of BCP rats, netrin-1 might be secreted by differentiated osteoclasts, resulting in the heightened innervation of CGRP + nociceptive nerve fibers.

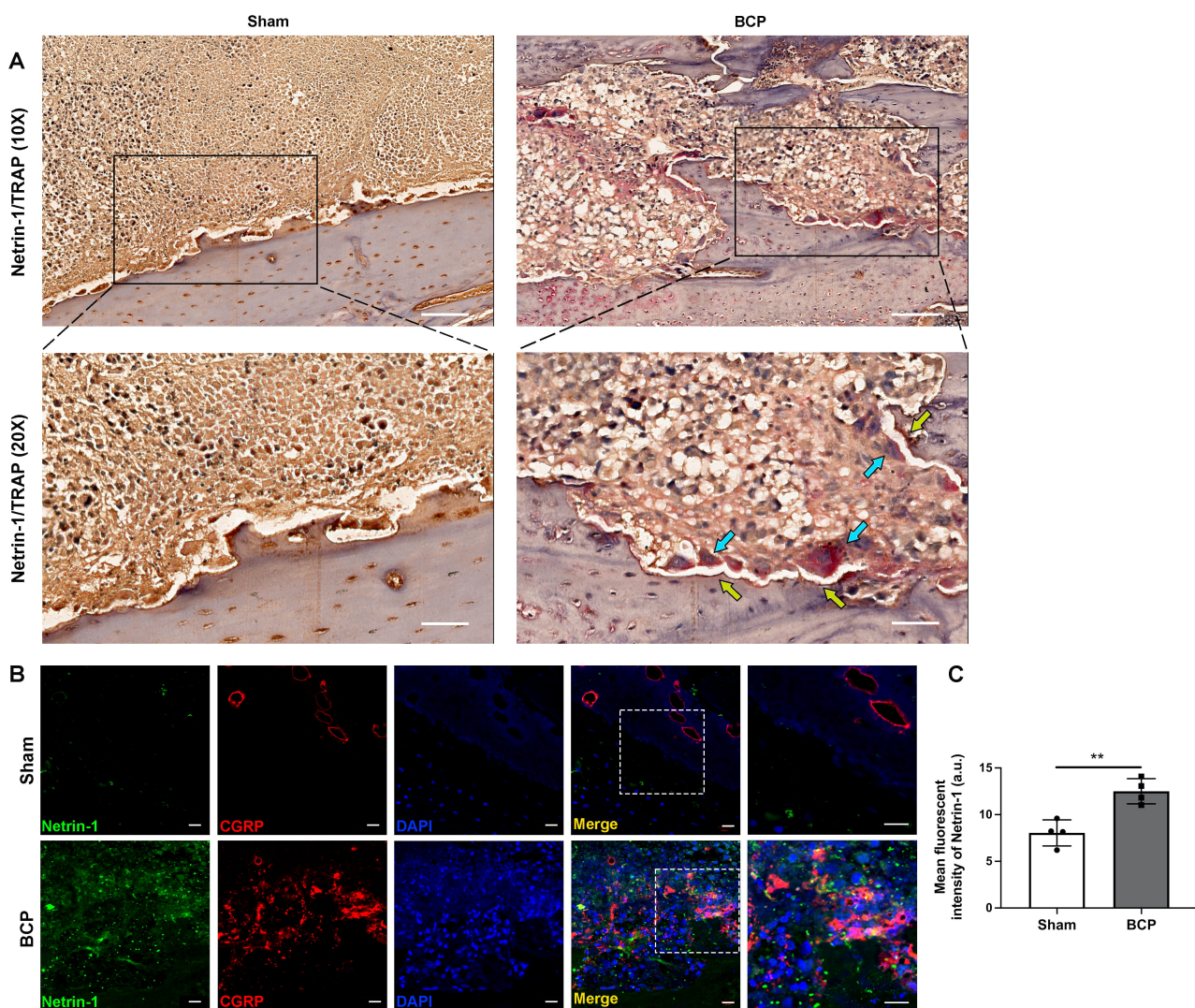


Fig. 3. Increased osteoclast-derived netrin-1 was related to the sprouting of nociceptive nerve fibers in the tibias of BCP rats. (A) Representative images of immunohistochemistry staining of netrin-1 (yellow arrows) and TRAP + osteoclasts (blue arrows) in the affected tibias of sham-treated and BCP rats on day 21, n = 4 per group. Scale bars, 200 μm (10×); 100 μm (20×). (B) Double immunofluorescence of netrin-1 and CGRP in the affected tibias of sham-treated and BCP rats on day 21. Scale bars: 20 μm. (C) Quantitative analysis of the mean density of netrin-1 in panel B, n = 4 per group. Data are expressed as mean ± SD. **p < 0.01. DAPI, 4',6-diamidino-2-phenylindole.

3.4 Netrin-1 Induces Sprouting of Peripheral CGRP + Fibers in BCP Progression through DCC/FAK/Rac1/Cdc42 Signaling Pathway

We examined the expressions of the receptors of netrin-1 in the ipsilateral DRG, and the results demonstrated that the transcription of DCC mRNA (Fig. 4A), rather than that of UNC5B mRNA (Fig. 4B), was significantly upregulated in BCP rats compared to sham-treated rats. Consistently, western blotting showed upregulation of DCC expression in the DRG of BCP rats. In contrast, the expression of UNC5B was not significantly altered (Fig. 4C). In addition, downstream signals of netrin-1/DCC signaling were further verified by examining the phosphorylation levels of FAK and Rac1/Cdc42 in BCP rats. The results indi-

cated that phosphorylation of FAK and following phosphorylation of Rac1/Cdc42 were significantly upregulated in BCP rats compared to the sham-treated group (Fig. 4C). Moreover, immunofluorescent staining showed prominent upregulation of DCC expression in the affected tibias of BCP rats compared with sham-treated rats (Fig. 4D,E). Double immunofluorescent staining showed evident colocalization of DCC and CGRP in the affected tibias of BCP rats (Fig. 4D). The findings suggest that netrin-1 may control nerve regeneration through the DCC receptor and its associated downstream signals, promoting the development of BCP.

To further elucidate the role of activated netrin-1/DCC signaling during BCP hypersensitivity, DCC was knocked

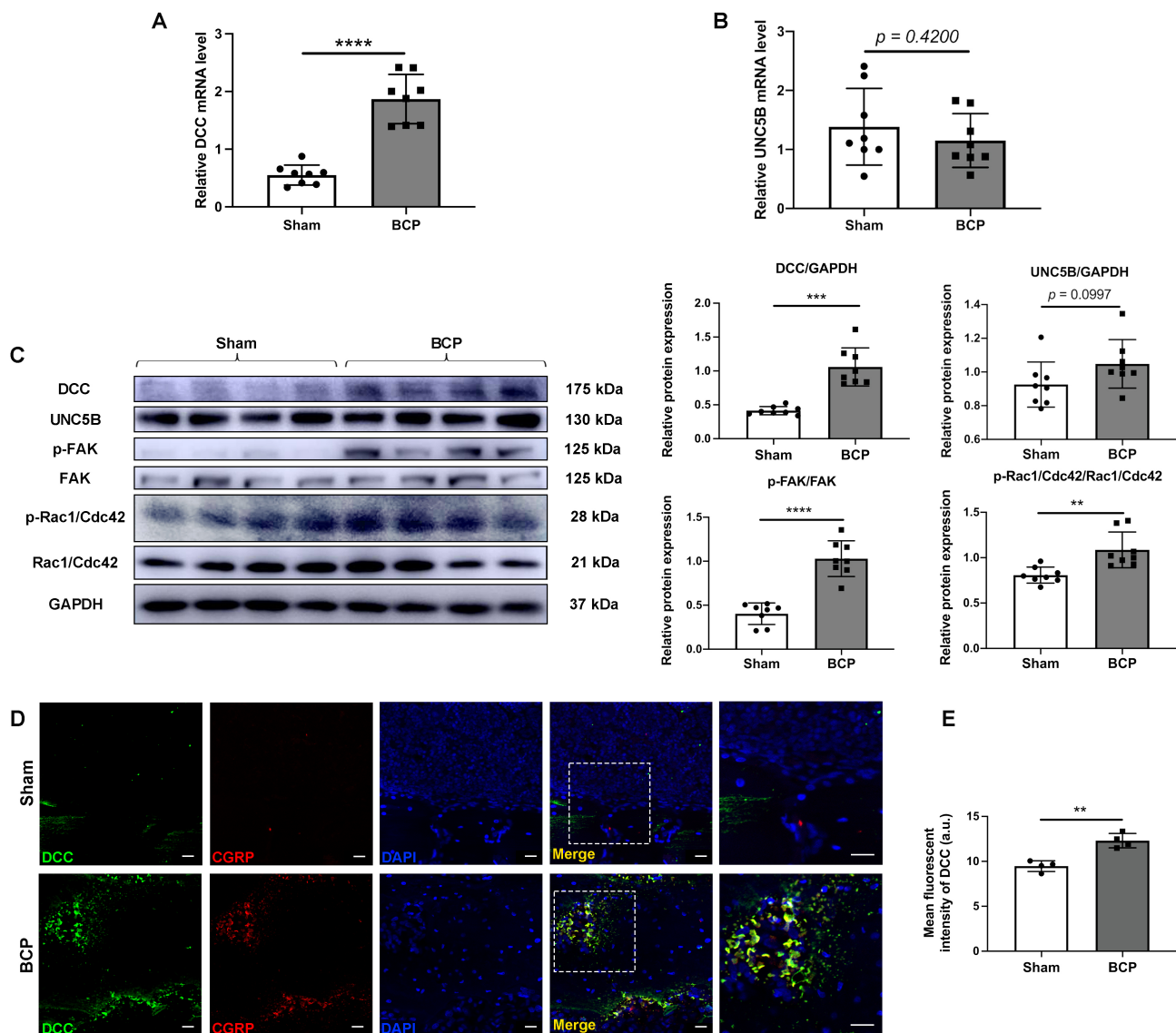


Fig. 4. Netrin-1 contributed to the sprouting of sensory nerve fiber in the metastatic bone lesions through the netrin-1/DCC signaling pathway. RT-qPCR analysis of the expression of (A) DCC and (B) UNC5B in the DRG on day 21. $n = 8$ per group. (C) The expressions of DCC, UNC5B, and phosphorylation levels of FAK and Rac1/Cdc42 in the DRG of rats in the sham and BCP groups on day 21 were determined by western blotting with representative protein bands presented. GAPDH was detected as an internal control. $n = 8$ per group. (D) Double immunofluorescence of DCC and CGRP in the affected tibias of sham-treated and BCP rats on day 21. Scale bars: 20 μm . (E) Quantitative analysis of the mean density of DCC. $n = 4$ per group. Data are expressed as mean \pm SD. $**p < 0.01$, $***p < 0.001$, $****p < 0.0001$. RT-qPCR, Real-Time Quantitative PCR; DCC, deleted in colorectal cancer; DRG, dorsal root ganglia; FAK, focal adhesion kinase; GAPDH, glyceraldehyde-3-phosphate dehydrogenase.

down by siRNA in BCP rats *in vivo*. DCC siRNA or vehicle were intrathecally injected on days 10, 13, and 16 after BCP model establishment. Pain behavior tests were conducted immediately prior to the start of the experiment, on the first day of treatment, and then daily during the treatment period (Fig. 5A). Targeting by siRNA significantly reduced DCC mRNA transcription (Supplementary Fig. 1) and inhibited the downstream phosphorylation levels of FAK and Rac1/Cdc42 (Fig. 5B). Meanwhile, we detected a significantly decreased innervation of CGRP + nociceptive nerve

fibers in the affected tibias (Fig. 5C,D). As anticipated, the rats exhibited a reduction in mechanical pain-related behaviors, as evidenced by the enhancement of PWMT levels and limb utilization (Fig. 5E,F), from day 11 to day 17 following intrathecal siRNA administration. These findings demonstrate that DCC signaling is essential in controlling peripheral nociceptive nerve innervation and plays a crucial role in developing and maintaining bone cancer pain.

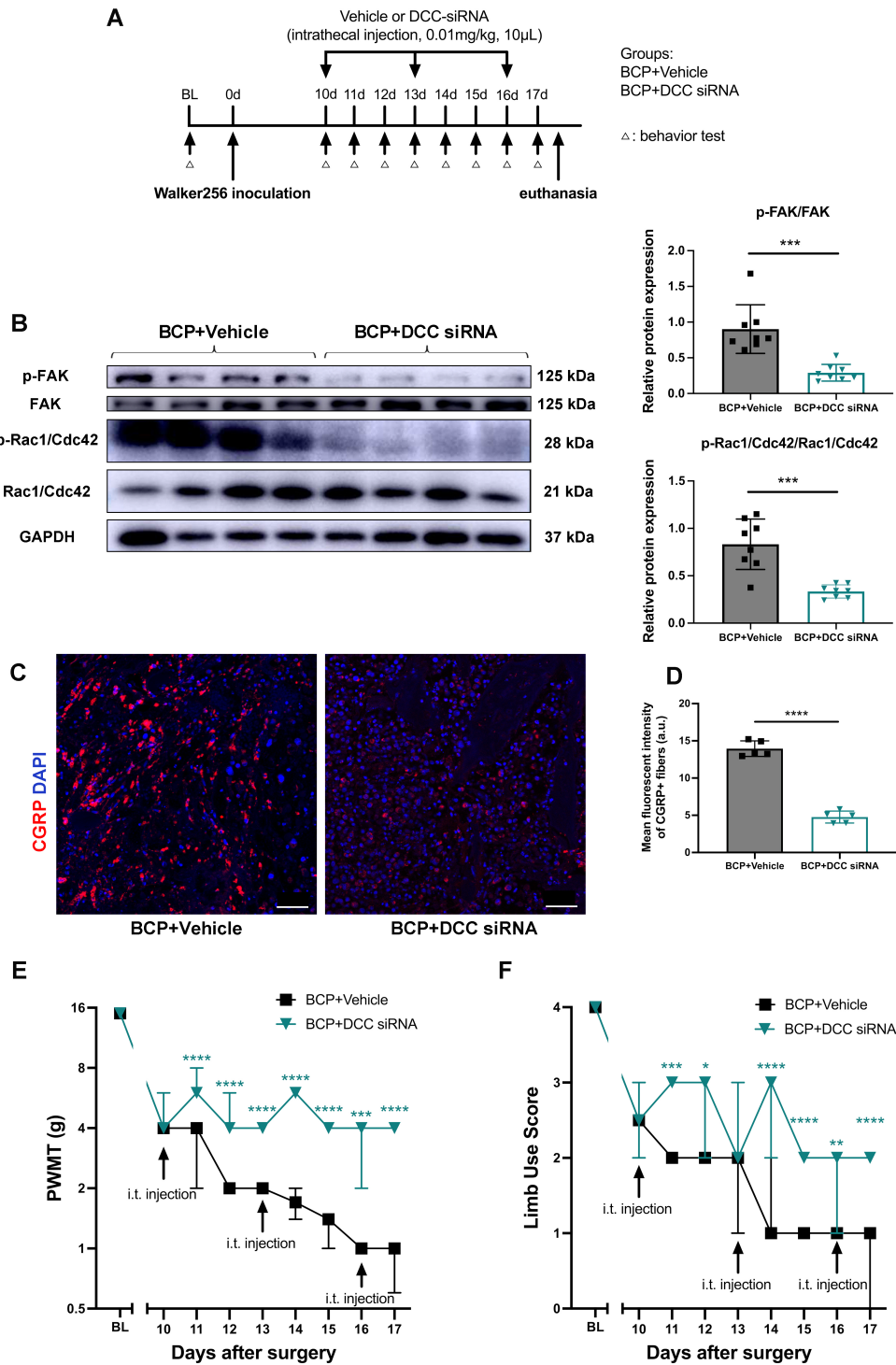


Fig. 5. Targeting DCC by intrathecal siRNAs administration in BCP rats. (A) Timeline of the experimental schedule for siRNA or vehicle injections. (B) Expressions of p-FAK/FAK and p-Rac1/Cdc42/Rac1/Cdc42 in the DRG of BCP rats treated with intrathecal vehicle or DCC-siRNA administration were determined by western blotting with representative protein bands presented. GAPDH was detected as an internal control. $n = 8$ per group. Data are expressed as mean \pm SD. $***p < 0.001$. (C) Representative immunofluorescent photomicrographs of CGRP + sensory nerve fibers (red) in the affected bones after intrathecal DCC siRNA or vehicle administration. Scale bars, 50 μ m. (D) Quantitative analysis of the density of CGRP + sensory nerve fibers in the affected tibias. $n = 5$ per group. Data are expressed as mean \pm SD. $****p < 0.0001$. (E) Paw withdrawal mechanical threshold (PWMT) and (F) limb use score were measured on the days of treatment, immediately prior to receiving DCC siRNA or vehicle administration, and daily after treatment in BCP rats, $n = 12$ per group. Data are expressed as median \pm 95% CI. $*p < 0.05$, $**p < 0.01$, $***p < 0.001$, $****p < 0.0001$.

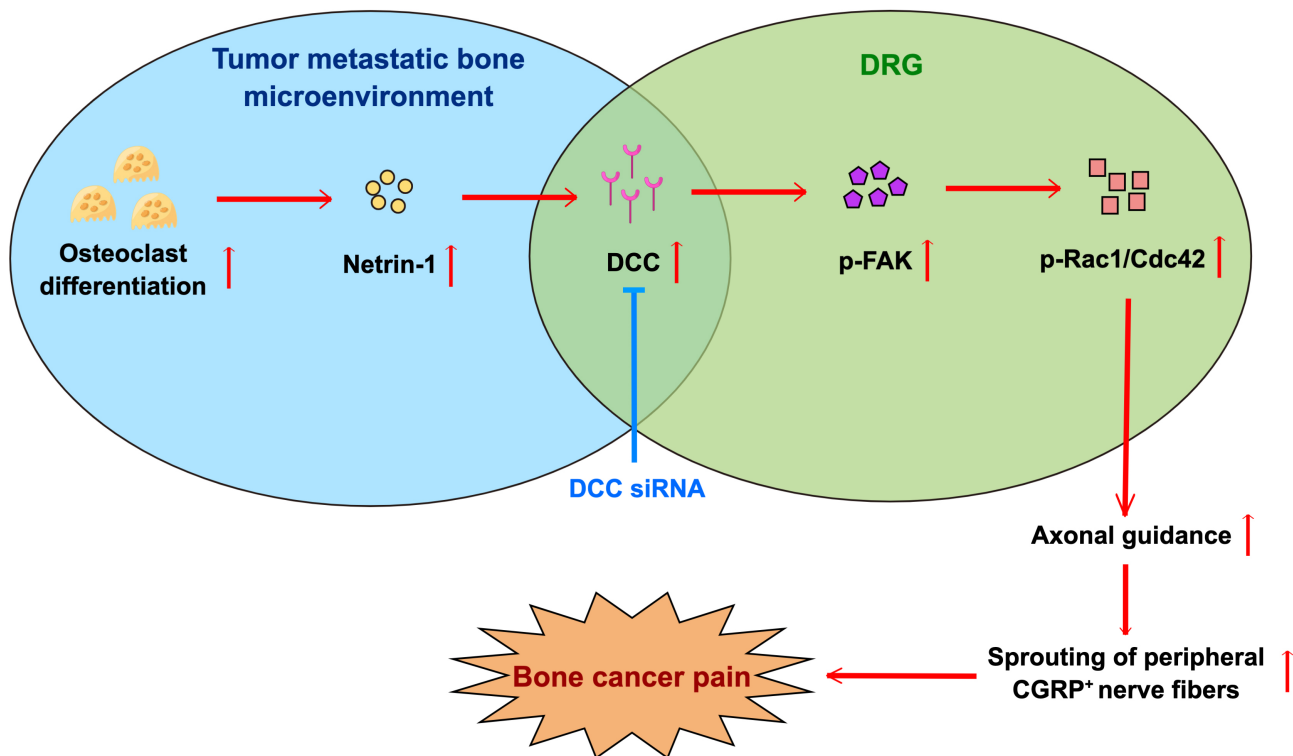


Fig. 6. Schematic summary of the mechanism by which netrin-1/DCC signaling aggravates bone cancer pain. Expression of netrin-1 in the metastatic bone lesion was significantly increased, subsequently activating netrin-1/DCC/FAK/Rac1/Cdc42 signaling pathway to promote its biofunction on axonal guidance, thus promoting the innervation of peripheral CGRP + nerve fibers and eventually aggravated bone cancer pain. Intrathecal injection of DCC siRNA blocked the signal transduction of DCC signaling and was efficacious in alleviating bone cancer pain. This figure was created on Figdraw (<https://www.figdraw.com/#/>).

4. Discussion

The present study has identified for the first time the essential role of netrin-1 in mediating BCP by increasing the innervation of peripheral CGRP + nociceptive nerve fibers in BCP rats through the netrin-1/DCC signaling pathway. Specifically, we observed elevated innervation of CGRP + nociceptive nerve fibers in the affected tibias of BCP rats. Activated osteoclasts and netrin-1 expression increased in the metastatic bone lesions, demonstrating a spatial correlation with the heightened presence of CGRP + nociceptive nerve fibers. Conversely, the DRG of BCP rats displayed elevated expressions of DCC and its downstream signals. Furthermore, DCC expression in the metastatic site was also enhanced and colocalized with the increased CGRP + nerve fibers. Notably, the intrathecal administration of DCC siRNA yielded a significant reduction in downstream signal expressions, peripheral CGRP + nociceptive nerve innervation, and ultimately alleviated pain behaviors in BCP rats (Fig. 6).

The initiation of BCP is a complex process. Sprouting of nociceptive nerve fibers is believed to be closely related to BCP development [36–40]. Following injury or disease, various factors and axon guidance molecules released by stromal and inflammatory cells can potentially induce

the sprouting of peripheral nociceptive nerve fibers, resulting in heightened sensitivity of the metastatic bone lesion, thereby exacerbating bone cancer pain. Furthermore, our previous investigation demonstrated that excessive activation of bone morphogenetic protein-2 (BMP2) represents a crucial step in the mechanism of peripheral sensitization of bone cancer pain [41]. On the other hand, BMP2 is believed to be closely related to early axonal regrowth after nerve injury [42,43]. Overall, this evidence shows that controlling bone remodeling and nociceptive nerve innervation is crucial for the occurrence and development of pain sensation during bone metastases of tumors. Recently, studies have confirmed the importance of netrin-1, one of the direct modulators of neurite elongation, in modulating pain development by regulating neurite elongation [22].

In the present study, netrin-1 expression in the affected bone of BCP rats was higher than that in the sham group. In BCP development, the netrin-1 receptor DCC is upregulated in the ipsilateral DRG rather than UNC5B. CGRP is spatially proximal to netrin-1 in BCP rats and colocalized with DCC in the affected tibias. Targeting DCC through intrathecal injection of siRNA significantly reduced the innervation of CGRP + nociceptive nerve fibers in the affected bone and improved pain behaviors in BCP rats.

Moreover, multiple studies have reported that focal adhesion kinase (FAK), a subtype of protein tyrosine kinases (PTKs), is activated by netrin-1/DCC signaling in the neurons of the corpus callosum, which plays an important part in axonal formation and elongation [44–47]. Recently, Ye *et al.* [48] reported that netrin-1 activates the cytoskeletal regulator Rac1/Cdc42 and downstream kinase Pak1 by binding to DCC, thereby inducing growth cone expansion and neurite elongation. There was a significant increase in p-FAK and p-Rac1/Cdc42 in the ipsilateral DRG of BCP rats. Intrathecal injection of DCC-siRNA notably inhibited the phosphorylation levels of FAK and Rac1/Cdc42. In line with this evidence, the current study identified the potential role of netrin-1 in the BCP development by inducing abnormal sprouting of nociceptive CGRP + neurite through netrin-1/DCC and its downstream FAK/Rac1/Cdc42 signaling pathway.

As reported, macrophage-derived netrin-1 is a crucial factor that promotes neurite growth and sensitization through the upregulation of CGRP in endometriosis [26]. Additionally, senescent fibroblast cell-secreted netrin-1 has been demonstrated to significantly modulate aging-related diseases by recruiting sympathetic fibers [27]. Last, netrin-1 secreted by osteoclasts in osteoarthritis is convinced to participate in augmented sensory innervation and osteoarthritis pain [22]. The enrichment of netrin-1 in various locations is crucial for neurite elongation and body function modification. In our study, we observed significant upregulation of osteoclast-derived netrin-1 only in affected bone tissues of BCP rat models. However, whether other sources of netrin-1 synthesis and secretion are associated with BCP progression still needs to be confirmed.

There are several limitations to this study. One aspect to consider is that all experiments were conducted using female rats due to the utilization of Walker256 breast cancer cells to establish the BCP model. Existing literature indicates that sex hormones, such as estrogen or testosterone, may influence pain phenotypes [49,50]. To mitigate gender-related bias, we opted to use female rats in this study exclusively. However, further research is warranted to explore the role of netrin-1/DCC signaling in the development of BCP in other gender, species, or BCP models established using different cell lines, such as MDAMB231 cancer cells or SHZ-88 cancer cells. Furthermore, recent investigations have indicated that the netrin-1/DCC signaling pathway positively impacts peripheral nerve regeneration [51]. Therefore, when considering the therapeutic potential of netrin-1 and its downstream signaling in managing BCP, it is crucial to account for its dual functionality.

Moreover, netrin-1 is reported to be associated with inhibiting tumor growth and metastasis through netrin-1/UNC5B signaling [52]. Whether upregulated netrin-1 in the metastatic bone microenvironment ameliorates BCP through this mechanism needs further investigation. As for the methodology, additional applications of other tech-

nologies and devices, such as electrophysiological recording, dynamic weight-bearing (DWB) systems, and other behavioral tests, may help identify different pain phenotypes [53]. Lastly, BCP is a complex complication of advanced metastatic bone cancer with intricate and complicated mechanisms. Netrin-1/DCC signaling is a potential therapeutic target for BCP. More molecules and signaling pathways, such as GFAP, IBA-1, or glutamate, need to be confirmed to provide new insights for BCP management.

Despite the limitations discussed above and given the increasing incidence of bone metastases of tumors and the inadequate control of BCP by existing available medication, a better understanding of BCP mechanisms would potentially help discover more effective analgesics. Our study has determined that netrin-1/DCC signaling is essential in remodeling nociceptive nerve innervation of metastatic bone lesions during BCP development. Inhibition of netrin-1/DCC signaling reduces innervation of nociceptive nerve fibers and ameliorates pain behaviors at the onset of bone metastasis of tumors; therefore, it may have therapeutic potential for BCP management.

5. Conclusions

The findings highlighted for the first time that the activation of netrin-1/DCC signaling may contribute to bone cancer pain in rats by increasing the innervation of peripheral CGRP + nociceptive nerve fibers. These observations may provide a novel strategy for studying and managing bone cancer pain.

Availability of Data and Materials

The datasets used and/or analyzed during the current study are available from the corresponding author on reasonable request.

Author Contributions

ZG, WW, XY and JW designed the research study. ZG, YZ, XL and KW performed the research. JW and XY gave experimental technical guidance. ZG and YZ analyzed the data. ZG wrote the manuscript. All authors contributed to editorial changes in the manuscript. All authors read and approved the final manuscript. All authors have participated sufficiently in the work and agreed to be accountable for all aspects of the work.

Ethics Approval and Consent to Participate

All experiments were performed in accordance with protocols approved by the Animal Care and Use Committee of Shanghai Chest Hospital, Shanghai Jiao Tong University, School of Medicine [Permission No. KS (Y)20186].

Acknowledgment

The authors would like to express their gratitude to EditSprings for the expert linguistic services provided.

Funding

This work was supported by the National Natural Science Foundation of China (82071233) and the Shanghai Sailing Program (21YF1442900).

Conflict of Interest

The authors declare no conflict of interest.

Supplementary Material

Supplementary material associated with this article can be found, in the online version, at <https://doi.org/10.31083/j.jin2303047>.

References

- [1] Aielli F, Ponzetti M, Rucci N. Bone Metastasis Pain, from the Bench to the Bedside. *International Journal of Molecular Sciences*. 2019; 20: 280.
- [2] Mercadante S. Malignant bone pain: pathophysiology and treatment. *Pain*. 1997; 69: 1–18.
- [3] Mantyh P. Bone cancer pain: causes, consequences, and therapeutic opportunities. *Pain*. 2013; 154: S54–S62.
- [4] Desandre PL, Quest TE. Management of cancer-related pain. *Emergency Medicine Clinics of North America*. 2009; 27: 179–194.
- [5] Zajączkowska R, Kocot-Kępska M, Leppert W, Wordliczek J. Bone Pain in Cancer Patients: Mechanisms and Current Treatment. *International Journal of Molecular Sciences*. 2019; 20: 6047.
- [6] Jimenez-Andrade JM, Bloom AP, Stake JJ, Mantyh WG, Taylor RN, Freeman KT, *et al.* Pathological sprouting of adult nociceptors in chronic prostate cancer-induced bone pain. *The Journal of Neuroscience*. 2010; 30: 14649–14656.
- [7] Mantyh WG, Jimenez-Andrade JM, Stake JJ, Bloom AP, Kaczmarek MJ, Taylor RN, *et al.* Blockade of nerve sprouting and neuroma formation markedly attenuates the development of late stage cancer pain. *Neuroscience*. 2010; 171: 588–598.
- [8] Hansen RR, Vacca V, Pitcher T, Clark AK, Malcangio M. Role of extracellular calcitonin gene-related peptide in spinal cord mechanisms of cancer-induced bone pain. *Pain*. 2016; 157: 666–676.
- [9] Chartier SR, Mitchell SAT, Majuta LA, Mantyh PW. The Changing Sensory and Sympathetic Innervation of the Young, Adult and Aging Mouse Femur. *Neuroscience*. 2018; 387: 178–190.
- [10] Jimenez-Andrade JM, Mantyh WG, Bloom AP, Xu H, Ferng AS, Dussor G, *et al.* A phenotypically restricted set of primary afferent nerve fibers innervate the bone versus skin: therapeutic opportunity for treating skeletal pain. *Bone*. 2010; 46: 306–313.
- [11] Mach DB, Rogers SD, Sabino MC, Luger NM, Schwei MJ, Pomonis JD, *et al.* Origins of skeletal pain: sensory and sympathetic innervation of the mouse femur. *Neuroscience*. 2002; 113: 155–166.
- [12] Averill S, McMahon SB, Clary DO, Reichardt LF, Priestley JV. Immunocytochemical localization of trkA receptors in chemically identified subgroups of adult rat sensory neurons. *The European Journal of Neuroscience*. 1995; 7: 1484–1494.
- [13] Selvaraj D, Gangadharan V, Michalski CW, Kurejova M, Stösser S, Srivastava K, *et al.* A Functional Role for VEGFR1 Expressed in Peripheral Sensory Neurons in Cancer Pain. *Cancer Cell*. 2015; 27: 780–796.
- [14] Wu CH, Yuan XC, Gao F, Li HP, Cao J, Liu YS, *et al.* Netrin-1 Contributes to Myelinated Afferent Fiber Sprouting and Neuropathic Pain. *Molecular Neurobiology*. 2016; 53: 5640–5651.
- [15] Madison RD, Zomorodi A, Robinson GA. Netrin-1 and peripheral nerve regeneration in the adult rat. *Experimental Neurology*. 2000; 161: 563–570.
- [16] Keino-Masu K, Masu M, Hinck L, Leonardo ED, Chan SS, Cullotti JG, *et al.* Deleted in Colorectal Cancer (DCC) encodes a netrin receptor. *Cell*. 1996; 87: 175–185.
- [17] Lai Wing Sun K, Correia JP, Kennedy TE. Nettrins: versatile extracellular cues with diverse functions. *Development*. 2011; 138: 2153–2169.
- [18] Wang Y, Teng HL, Huang ZH. Repulsive migration of Schwann cells induced by Slit-2 through Ca²⁺-dependent RhoA-myosin signaling. *Glia*. 2013; 61: 710–723.
- [19] Liu Y, Stein E, Oliver T, Li Y, Brunken WJ, Koch M, *et al.* Novel role for Nettrins in regulating epithelial behavior during lung branching morphogenesis. *Current Biology*. 2004; 14: 897–905.
- [20] Tu T, Zhang C, Yan H, Luo Y, Kong R, Wen P, *et al.* CD146 acts as a novel receptor for netrin-1 in promoting angiogenesis and vascular development. *Cell Research*. 2015; 25: 275–287.
- [21] Podjaski C, Alvarez JI, Bourbonniere L, Larouche S, Terouz S, Bin JM, *et al.* Netrin 1 regulates blood-brain barrier function and neuroinflammation. *Brain*. 2015; 138: 1598–1612.
- [22] Zhu S, Zhu J, Zhen G, Hu Y, An S, Li Y, *et al.* Subchondral bone osteoclasts induce sensory innervation and osteoarthritis pain. *The Journal of Clinical Investigation*. 2019; 129: 1076–1093.
- [23] Ni S, Ling Z, Wang X, Cao Y, Wu T, Deng R, *et al.* Sensory innervation in porous endplates by Netrin-1 from osteoclasts mediates PGE₂-induced spinal hypersensitivity in mice. *Nature Communications*. 2019; 10: 5643.
- [24] Watanabe K, Tamamaki N, Furuta T, Ackerman SL, Ikenaka K, Ono K. Dorsally derived netrin 1 provides an inhibitory cue and elaborates the ‘waiting period’ for primary sensory axons in the developing spinal cord. *Development*. 2006; 133: 1379–1387.
- [25] Masuda T, Watanabe K, Sakuma C, Ikenaka K, Ono K, Yaginuma H. Netrin-1 acts as a repulsive guidance cue for sensory axonal projections toward the spinal cord. *The Journal of Neuroscience*. 2008; 28: 10380–10385.
- [26] Guo X, Ding S, Li T, Wang J, Yu Q, Zhu L, *et al.* Macrophage-derived netrin-1 is critical for neuroangiogenesis in endometriosis. *International Journal of Biological Macromolecules*. 2020; 148: 226–237.
- [27] Yu AQ, Wang J, Zhou XJ, Chen KY, Cao YD, Wang ZX, *et al.* Senescent Cell-Secreted Netrin-1 Modulates Aging-Related Disorders by Recruiting Sympathetic Fibers. *Frontiers in Aging Neuroscience*. 2020; 12: 507140.
- [28] Dun XP, Parkinson DB. Role of Netrin-1 Signaling in Nerve Regeneration. *International Journal of Molecular Sciences*. 2017; 18: 491.
- [29] Ren XR, Ming GL, Xie Y, Hong Y, Sun DM, Zhao ZQ, *et al.* Focal adhesion kinase in netrin-1 signaling. *Nature Neuroscience*. 2004; 7: 1204–1212.
- [30] Li X, Saint-Cyr-Proulx E, Aktories K, Lamarche-Vane N. Rac1 and Cdc42 but not RhoA or Rho kinase activities are required for neurite outgrowth induced by the Netrin-1 receptor DCC (deleted in colorectal cancer) in N1E-115 neuroblastoma cells. *The Journal of Biological Chemistry*. 2002; 277: 15207–15214.
- [31] Zimmermann M. Ethical guidelines for investigations of experimental pain in conscious animals. *Pain*. 1983; 16: 109–110.
- [32] Medhurst SJ, Walker K, Bowes M, Kidd BL, Glatt M, Muller M, *et al.* A rat model of bone cancer pain. *Pain*. 2002; 96: 129–140.
- [33] Remeniuk B, Sukhtankar D, Okun A, Navratilova E, Xie JY, King T, *et al.* Behavioral and neurochemical analysis of ongoing bone cancer pain in rats. *Pain*. 2015; 156: 1864–1873.
- [34] Livak KJ, Schmittgen TD. Analysis of relative gene expression data using real-time quantitative PCR and the 2⁻(Delta Delta C(T)) Method. *Methods*. 2001; 25: 402–408.

- [35] Yuan X, Qian N, Ling S, Li Y, Sun W, Li J, *et al.* Breast cancer exosomes contribute to pre-metastatic niche formation and promote bone metastasis of tumor cells. *Theranostics*. 2021; 11: 1429–1445.
- [36] Mantyh PW. Mechanisms that drive bone pain across the lifespan. *British Journal of Clinical Pharmacology*. 2019; 85: 1103–1113.
- [37] Xiang L, Gilkes DM. The Contribution of the Immune System in Bone Metastasis Pathogenesis. *International Journal of Molecular Sciences*. 2019; 20: 999.
- [38] Brodowicz T, O’Byrne K, Manegold C. Bone matters in lung cancer. *Annals of Oncology: Official Journal of the European Society for Medical Oncology*. 2012; 23: 2215–2222.
- [39] Tahara RK, Brewer TM, Theriault RL, Ueno NT. Bone Metastasis of Breast Cancer. *Advances in Experimental Medicine and Biology*. 2019; 1152: 105–129.
- [40] Hiraga T. Bone metastasis: Interaction between cancer cells and bone microenvironment. *Journal of Oral Biosciences*. 2019; 61: 95–98.
- [41] Wang W, Jiang Q, Wu J, Tang W, Xu M. Upregulation of bone morphogenetic protein 2 (Bmp2) in dorsal root ganglion in a rat model of bone cancer pain. *Molecular Pain*. 2019; 15: 1744806918824250.
- [42] Ma CHE, Brenner GJ, Omura T, Samad OA, Costigan M, Inquimbert P, *et al.* The BMP coreceptor RGMB promotes while the endogenous BMP antagonist noggin reduces neurite outgrowth and peripheral nerve regeneration by modulating BMP signaling. *The Journal of Neuroscience*. 2011; 31: 18391–18400.
- [43] Wu G, Ju L, Jin T, Chen L, Shao L, Wang Y, *et al.* Local delivery of recombinant human bone morphogenetic protein-2 increases axonal regeneration and the expression of tau protein after facial nerve injury. *The Journal of International Medical Research*. 2010; 38: 1682–1688.
- [44] Moore SW, Zhang X, Lynch CD, Sheetz MP. Netrin-1 attracts axons through FAK-dependent mechanotransduction. *The Journal of Neuroscience*. 2012; 32: 11574–11585.
- [45] Lv J, Sun X, Ma J, Ma X, Zhang Y, Li F, *et al.* Netrin-1 induces the migration of Schwann cells via p38 MAPK and PI3K-Akt signaling pathway mediated by the UNC5B receptor. *Biochemical and Biophysical Research Communications*. 2015; 464: 263–268.
- [46] Boyer NP, Gupton SL. Revisiting Netrin-1: One Who Guides (Axons). *Frontiers in Cellular Neuroscience*. 2018; 12: 221.
- [47] Brudvig JJ, Cain JT, Schmidt-Grimminger GG, Stumpo DJ, Roux KJ, Blackshear PJ, *et al.* MARCKS Is Necessary for Netrin-DCC Signaling and Corpus Callosum Formation. *Molecular Neurobiology*. 2018; 55: 8388–8402.
- [48] Ye X, Qiu Y, Gao Y, Wan D, Zhu H. A Subtle Network Mediating Axon Guidance: Intrinsic Dynamic Structure of Growth Cone, Attractive and Repulsive Molecular Cues, and the Intermediate Role of Signaling Pathways. *Neural Plasticity*. 2019; 2019: 1719829.
- [49] Lee JY, Choi HY, Ju BG, Yune TY. Estrogen alleviates neuropathic pain induced after spinal cord injury by inhibiting microglia and astrocyte activation. *Biochimica et Biophysica Acta. Molecular Basis of Disease*. 2018; 1864: 2472–2480.
- [50] Choi JC, Park YH, Park SK, Lee JS, Kim J, Choi JI, *et al.* Testosterone effects on pain and brain activation patterns. *Acta Anaesthesiologica Scandinavica*. 2017; 61: 668–675.
- [51] Ke X, Li Q, Xu L, Zhang Y, Li D, Ma J, *et al.* Netrin-1 overexpression in bone marrow mesenchymal stem cells promotes functional recovery in a rat model of peripheral nerve injury. *Journal of Biomedical Research*. 2015; 29: 380–389.
- [52] Sung PJ, Rama N, Imbach J, Fiore S, Ducarouge B, Neves D, *et al.* Cancer-Associated Fibroblasts Produce Netrin-1 to Control Cancer Cell Plasticity. *Cancer Research*. 2019; 79: 3651–3661.
- [53] Guida F, De Gregorio D, Palazzo E, Ricciardi F, Boccella S, Belardo C, *et al.* Behavioral, Biochemical and Electrophysiological Changes in Spared Nerve Injury Model of Neuropathic Pain. *International Journal of Molecular Sciences*. 2020; 21: 3396.